



the society for solid-state
and electrochemical
science and technology

Journal of The Electrochemical Society

Realizing the Performance of LiCoPO_4 Cathodes by Fe Substitution with Off-Stoichiometry

S. M. G. Yang, V. Aravindan, W. I. Cho, D. R. Chang, H. S. Kim and Y. S. Lee

J. Electrochem. Soc. 2012, Volume 159, Issue 7, Pages A1013-A1018.
doi: 10.1149/2.051207jes

Email alerting service

Receive free email alerts when new articles cite this article - sign up in the box at the top right corner of the article or [click here](#)

To subscribe to *Journal of The Electrochemical Society* go to:
<http://jes.ecsdl.org/subscriptions>



Realizing the Performance of LiCoPO₄ Cathodes by Fe Substitution with Off-Stoichiometry

S. M. G. Yang,^a V. Aravindan,^{a,b} W. I. Cho,^c D. R. Chang,^d H. S. Kim,^d and Y. S. Lee^{a,z}

^aFaculty of Applied Chemical Engineering, Chonnam National University, Gwang-ju 500-757, Korea

^bEnergy Research Institute (ERI@N), Nanyang Technological University, Research Techno Plaza, Singapore 637553, Singapore

^cEnergy and Environment Division, Korea Institute of Science and Technology, Seoul 136-791, Korea

^dKorea Institute of Industrial Technology, Gwang-ju 500-480, South Korea

Fe substituted lithium rich cobalt phosphates ($\text{Li}_{1+x}[\text{Co}_{1-y}\text{Fe}_y]_{1-x}\text{PO}_4$, $0 \leq x \leq 0.2$, $0 \leq y \leq 0.2$) were successfully synthesized by the solid-state reaction. Firstly, the optimization of appropriate temperature conditions (800, 850 and 900°C for 10 h) to yield the phase pure LiCoPO₄ was conducted. Based on the cell performance of LiCoPO₄ prepared aforementioned conditions, 800°C for 10 h calcinations condition was found better performance than rest. Lithium phases optimization was carried out and it was found that the cell performance obtained when the lithium content was 1.05 (real content is 1.02) was better than that of the stoichiometric and other lithium rich compositions prepared. Similarly, the substitution of Fe into the Co sites was also conducted for the lithium rich cobalt phosphate ($\text{Li}_{1.02}[\text{Co}_{0.9}\text{Fe}_{0.1}]_{0.98}\text{PO}_4$, $0 \leq y \leq 0.2$) and excellent cycling performance was obtained when the Fe content was 0.1 in conventional solutions. The X-ray diffraction pattern and Rietveld analysis showed that $\text{Li}_{1.02}[\text{Co}_{0.9}\text{Fe}_{0.1}]_{0.98}\text{PO}_4$ has a well-developed orthorhombic structure with *Pnma* space group. The lattice parameters of $\text{Li}_{1.02}[\text{Fe}_{0.1}\text{Co}_{0.9}]_{0.98}\text{PO}_4$ are slightly larger than those of LiCoPO₄ due to the larger ionic size of doped Fe²⁺ (0.78 Å) compared with Co²⁺ (0.745 Å). In conclusion, the $\text{Li}/\text{Li}_{1.02}[\text{Co}_{0.9}\text{Fe}_{0.1}]_{0.98}\text{PO}_4$ cell delivered an initial discharge capacity of 130 mAh g⁻¹ and retained 90% of its initial capacity (117 mAh g⁻¹) at the end of the 15th cycle at 0.1 C rate. We concluded that the substituted Li and Fe ions play an important role in enhancing the battery performance of the LiCoPO₄ material by improving the kinetics of the lithium insertion/extraction reaction on the electrode.

© 2012 The Electrochemical Society. [DOI: 10.1149/2.051207jes] All rights reserved.

Manuscript submitted January 23, 2012; revised manuscript received April 4, 2012. Published July 17, 2012.

Since the demonstration of the reversible insertion and extraction of lithium ions in polyanion framework materials (XO_4^{3-} , where X = P, Si, Mo and W, much attention has been paid toward the possibility of using them as cathode materials in lithium batteries.¹ Among them, olivine phosphates, LiMPO_4 (where M = Fe, Mn, Co and Ni), are noteworthy from the practical point of view, due to their salient features such as their better thermal stability than conventional cathodes (LiCoO₂ and LiMn₂O₄) owing to the presence of strong P–O bonding. They are also easy to prepare on an industrial scale, have very flat charge-discharge profiles, higher theoretical energy densities, etc.^{2–6} At the same time, however, all olivine phosphates suffer from inherent conducting properties. So far, the conductivity issue of electrode materials has been resolved by several approaches, such as the deposition of conductive coatings on the surface of the active particles (preferably by carbon coating),^{6–8} the isovalent or aliovalent doping on either lithium or transition metal sites⁹ and creating a rich or deficient phase of lithium.^{5,10,11} Electric and hybrid electric vehicle (EV and HEV) applications require a high practical energy density with size geometry. This requirement could be fulfilled by adopting high voltage cathodes in practical cells.

Recently, in 2006, one US venture company (A123 systems) commercialized high-power lithium-ion batteries with LiFePO₄/C nanocomposites for power tool applications¹² and later, in 2009, Sony announced the mass production of LiFePO₄ based batteries for the market,¹³ however the energy density of such cells is limited due to their restricted operating potential of 3.4 V vs. Li. The operating potential of the other olivine candidate, LiMnPO₄, is 0.7 V higher than that of the former (4.1 V vs. Li), however very few researchers have achieved the full performance of the material and this by adopting either carbon coating or fabricating composite electrodes.^{14–21} Furthermore, the operating potential is only ~0.7 V higher than that of LiFePO₄ cathodes and, hence, most research work has focused on other LiCoPO₄ olivine candidates.

Although LiCoPO₄ offers a high operating voltage (4.8 V vs. Li) and higher theoretical energy density (800 Wh kg⁻¹) than its counterparts in the olivine group, it has been less studied by researchers due to its low conductivity and poor compatibility with conventional electrolytes.^{3,22–28} In this situation, we started to optimize the synthe-

sis of this high voltage candidate for next generation lithium-ion cells in conventional electrolyte solutions.

Amine et al.²² firstly reported the reversible insertion and extraction of lithium ions in LiCoPO₄ with the presence of 1 M LiPF₆ in a sulfolane based electrolyte. The test cells delivered a discharge capacity of 70 mAh g⁻¹, which corresponds to 0.42 moles of Li per formula unit. Later, Yang et al.²⁹ attempted to form an in-situ carbon coating to improve the electronic conductivity and failed to make such a coating due to the peculiar surface properties of LiCoPO₄. However, Li et al.³⁰ succeeded in preparing carbon coated LiCoPO₄ by the incorporating acetylene black during the synthesis process. This approach provides a heterogeneous coating for the materials and leads to severe capacity fading. Moreover, this process required high temperature sintering in an inert atmosphere, which leads to the formation of secondary phase materials such as Co₂P. The appearance of such secondary phases is due to the high temperature sintering with carbon or its precursors in an inert atmosphere for a long duration. The formation of Co₂P is also sometimes beneficial for the improvement in the electronic conductivity of the material, as confirmed by Wolfenstine.³¹ Cation doping is one of the novel approaches to improve the electronic conductivity by four or five orders of magnitude in polyanion hosts, as confirmed by Chung et al.³² for the LiFePO₄ system. In the case of LiCoPO₄, an improvement in the electronic conductivity and improved kinetics properties were noted during Fe substitution into the Co sites, however no cycling profiles were reported. Herle et al.¹¹ adopted similar approach to create rich/deficient phases of lithium (non-stoichiometric) and aliovalent substitution into the lithium sites to improve the conductivity of olivine phosphates. Later, Kim et al.¹⁰ and Lee et al.⁵ demonstrated the improved electrochemical performance of the lithium rich phase, LiFePO₄, without any conductive coating. In this study, we attempted to create lithium rich cobalt phosphates and perform subsequent Fe doping into the cobalt sites to improve the electrochemical performance by enhancing the electronic conductivity. The optimizations of the synthesis temperature, lithium rich phase and cation doping are discussed in detail in a conventional electrolyte system.

Experimental

The conventional solid state method was employed to prepare and optimize the lithium cobalt phosphates. Stoichiometric proportions of

^zE-mail: leeys@chonnam.ac.kr

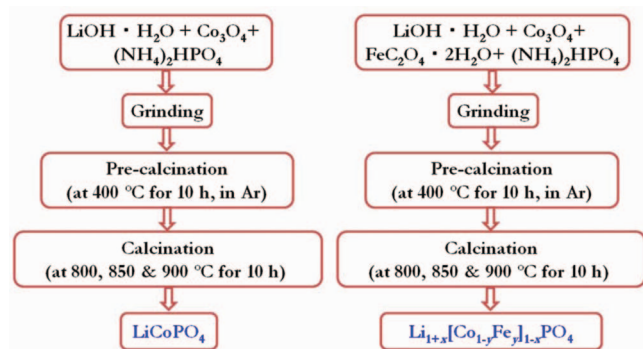


Figure 1. Schematic representation of the synthesis of lithium cobalt phosphates by solid-state reaction.

LiOH·H₂O (Junsei, Japan), Co₃O₄ (Aldrich, USA) C₆H₁₀O₄ (Aldrich, USA) and (NH₄)₂PO₄ (Sigma-Aldrich, USA) were used for the synthesis of LiCoPO₄. Initially, the preparatory materials were finely ground, made into a pellet, and heated at 400°C for 10 h to decompose the hydroxyl and ammonia moieties present in the source materials. The intermediate mixture was finely ground again, placed in a tubular furnace and heated at three different temperatures ranging from 800 to 900°C for 10 h to yield the resultant product. The tubular furnace was initially purged with Ar gas until the temperature reached the desired level (800°C) and then the flow of Ar was stopped. The presence of available carbon (derived from the carbonization of adipic acid) will reduce Co³⁺ to Co²⁺ carbothermally. Similar procedures were used for the preparation of the lithium rich and Fe substituted cobalt phosphates with appropriate proportions of starting materials based on the optimized temperature conditions. The synthesis procedure is schematically illustrated in Figure 1.

Thermal studies were conducted by means of thermogravimetric-differential thermal analysis (TG-DTA) using a thermal analyzer (STA 1640, Stanton Redcroft Inc., UK). In the TG-DTA measurement, the powders were heated at 5°C min⁻¹ and then cooled at 10°C min⁻¹. Structural characterizations were carried out by powder X-ray diffraction (XRD, Rint 1000, Rigaku, Japan) using CuK_α radiation. The Li, Co, and Fe concentrations in the resulting materials were analyzed using an inductively coupled plasma spectrometer (ICP, SPS 7800, Seiko Instruments, Japan). The cyclic voltammetric (CV) traces were recorded using a Bio-Logic electrochemical work station (SP-150, Biologic, France) with a three electrode cell configuration. In this configuration, metallic lithium served as the counter and reference electrodes. All of the electrochemical studies were performed using CR 2032 coin cells. The composite cathodes were formed with exactly 20 mg of the active material, 3 mg of ketzen black, and 3 mg of conductive binder (Teflonized acetylene black, TAB-2). It was pressed on a 200 mm² stainless steel mesh, which served as the current collector under a pressure of 300 kg cm⁻² and dried at 130°C for 5 hrs. The test cell was comprised of a composite cathode and metallic lithium as the anode separated by a porous polypropylene film (Celgard 3401, USA). 1 M LiPF₆ in an ethylene carbonate (EC)/dimethyl carbonate (DMC) (1:1 v/v, Techno Semichem Co., Ltd, Korea) mixture was used as the electrolyte for all of the studies. The galvanostatic cycling performances were recorded between 3.5–5.2 V with a constant current density of 0.1 C at room temperature.

Results and Discussion

Figure 2 represents the thermogravimetric-differential thermal analysis (TG-DTA) curves of the starting materials used for the synthesis of the lithium cobalt phosphate materials. The weight loss in the TGA curve at around ~150°C is ascribed to the removal of the hydroxyl groups and moisture present in the mixture during the loading of the sample. A gradual weight loss occurred up to 350°C, which may be ascribed to the removal of the ammonia moieties and the reac-

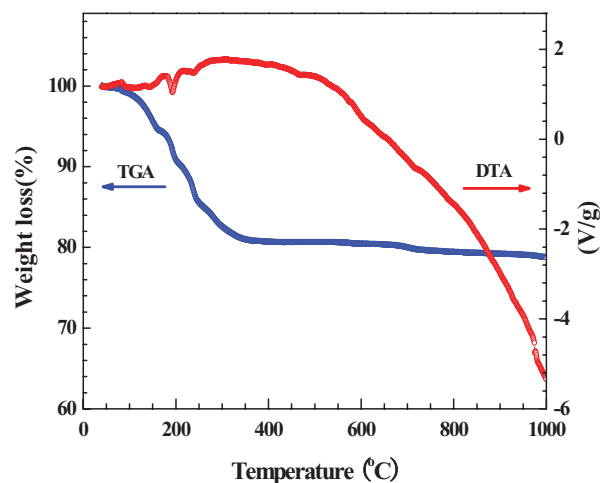


Figure 2. Thermogravimetric-differential thermal analyses (TG-DTA) traces of the starting materials used for the synthesis of LiCoPO₄.

tivity of the source materials. Also, a small thermal event is recorded at around ~650°C, which indicates the formation of LiCoPO₄ phase. Thereafter, there is no thermal event observed until 1000°C. The DTA curve also reflects the weight loss observed in the TGA analysis. Based on the thermal analyzes, we decided to calcine material at 800, 850 and 900°C to determine the optimum synthetic temperature of the LiCoPO₄ material.

Figure 3 presents the XRD patterns of the LiCoPO₄ materials prepared under the three different temperature conditions. The prepared LiCoPO₄ materials exhibited sharp intense reflections corresponding to their crystallite and phase pure nature. The observed patterns are consistent with JCPDS card (No. 89-6192) and the corresponding Bragg reflections are indexed according to an orthorhombic structure with *Pnma* space group. All of the XRD patterns are well developed and almost the same, which makes it very complicated to determine the optimum temperature for the preparation of LiCoPO₄. Hence, coin cells (Li/LiCoPO₄) were made to evaluate the electrochemical performance of the prepared cobalt phosphates at three different temperatures to finalize the optimum condition.

The electrochemical performances of the LiCoPO₄ samples prepared at three different temperatures are presented in Figure 4. All of the Li/LiCoPO₄ cells were cycled between 3.2 and 5.2 V at 0.1 C rate in conventional electrolyte conditions. The LiCoPO₄ prepared at 800°C presented a smoother discharge curve than those at the other temperatures (Fig. 4a) and showed better reversible capacity

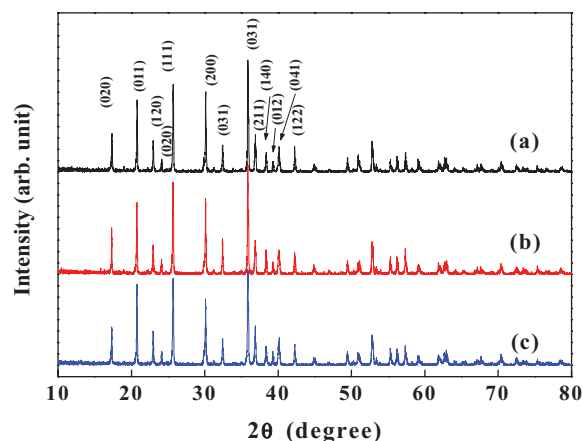


Figure 3. Powder X-ray diffraction patterns of LiCoPO₄ prepared at three different temperatures (a) 800°C, (b) 850°C and (c) 900°C.

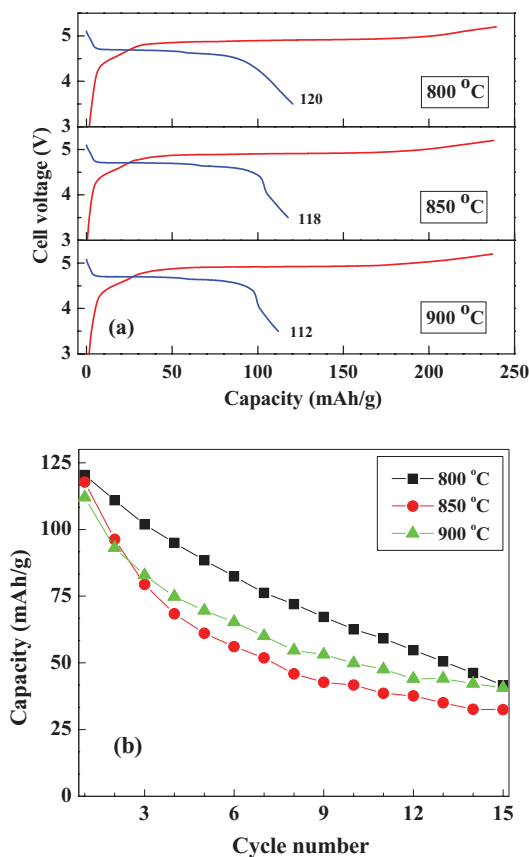


Figure 4. (a) Initial charge-discharge curves of Li/LiCoPO₄ cells recorded between 3.5–5.2 V at 0.1 C (800, 850 and 900 °C), (b) corresponding cycling profiles of the above cells at room temperature.

values (120 mAh g⁻¹) compared to the theoretical capacity of 167 mAh g⁻¹. It can be seen from the charge curves that the decomposition of the electrolyte occurs in all three prepared cells. The cycling profiles of the Li/LiCoPO₄ cells are illustrated in Figure 4b. It is quite obvious that capacity fading occurs in all three cells during the cycling process. This is ascribed to the poor electronic conducting nature of the materials prepared. Several researchers unsuccessfully attempted to make an in-situ carbon coating on the surface of the particles to improve the conductivity. However, Li et al.³⁰ prepared core-shell type LiCoPO₄ with carbon coating during the synthesis, but did not report on excellent cycleability. Moreover, this process can easily lead to the carbothermal reduction of LiCoPO₄ and the consequent formation of undetectable Co₂P impurities. Jin et al.³³ and Rabanal et al.³⁴ reported the synthesis of LiCoPO₄/C composites by high energy ball milling and their cycling profiles revealed severe capacity fading during the charge/discharge process. This clearly indicates that the inclusion of carbon and formation of the carbon-LiCoPO₄ composites does not improve the electrochemical performance of the cell during prolonged cycling. Hence, we attempted to prepare a new type of lithium cobalt phosphate material to improve the electronic conductivity of the LiCoPO₄, although the cycling profiles are also similar to those of either bare or composite LiCoPO₄.

In this regard, lithium rich phases of LiCoPO₄ were created to improve the conducting properties, as was convincingly proven by Lee et al.,⁵ Herle et al.,¹¹ and Kim et al.¹⁰ for the LiFePO₄ and Jang et al.³⁵ for LiCoPO₄ phases. Based on the comparison of the electrochemical performances of the LiCoPO₄ samples prepared at three different temperatures, it was decided to perform the heat-treatment at 800 °C for 10 h for the preparation of the remaining cobalt phosphates. Figure 5 represents the XRD patterns of the lithium rich cobalt phosphates (Li_{1+x}CoPO₄, 0 ≤ x ≤ 0.2) prepared at 800 °C. Three dif-

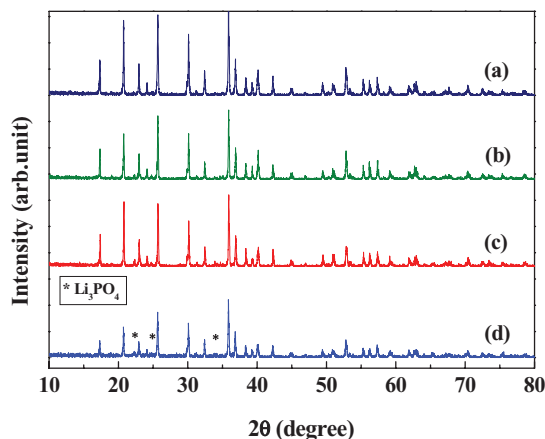


Figure 5. X-ray diffraction patterns of lithium rich cobalt phosphates (Li_{1+x}CoPO₄, 0 ≤ x ≤ 0.2) prepared at 800 °C, (a) LiCoPO₄, (b) Li_{1.05}CoPO₄, (c) Li_{1.1}CoPO₄ and (d) Li_{1.2}CoPO₄.

ferent proportions of the lithium rich cobalt phosphates were prepared along with the pristine material for comparison, namely, Li_{1.05}CoPO₄, Li_{1.1}CoPO₄ and Li_{1.2}CoPO₄ phases. The XRD reflections clearly indicate the formation of an orthorhombic structure. It is observed that increasing the concentration of lithium beyond the stoichiometric proportions leads to the formation of Li₃PO₄ as a secondary phase. The reflections at around 2θ = 22.4, 23.3 and 33.9 confirm the appearance of such a phase. The intensity of the Li₃PO₄ phase is increased with increasing lithium content beyond Li_{1.05}CoPO₄. Among the prepared lithium rich phase materials, only Li_{1.05}CoPO₄ material contained a negligible amount of Li₃PO₄ phase when compared to the rest of the compositions prepared. This study reveals that the preparation of pure Li_{1+x}CoPO₄ is very complicated, when compared to the Li_{1+x}FePO₄ system.

In order to estimate the effect of lithium rich content on the electrochemical performance of Li/Li_{1+x}CoPO₄ (0 ≤ x ≤ 0.2) cells, the samples were cycled between 3.5 and 5.2 V at 0.1 C rate. The charge/discharge and cycling profiles of the lithium rich cobalt phosphates are given in Figure 6. The Li/Li_{1+x}CoPO₄ cells delivered initial discharge capacities of 120, 123, 121 and 114 mAh g⁻¹ for LiCoPO₄, Li_{1.05}CoPO₄, Li_{1.1}CoPO₄ and Li_{1.2}CoPO₄ respectively. It is worth noticing that, except for the Li_{1.2}CoPO₄ phase, the other lithium rich materials exhibited almost the same discharge capacity behavior in the initial cycle. It is well known that, Li₃PO₄ is an excellent ionic conductor. Obvious to notice from the XRD patterns, trace amount of Li₃PO₄ impurity is exists when approaching beyond one mole of lithium in LiCoPO₄ phase. Hence the ionic conductivity of composite electrode has been improved. Increasing the molar concentration of lithium (> 1 mole), results in higher concentration of Li₃PO₄ phase which drastically increases the ionic conductivity, at the same time too much concentration of above phase suppresses the electronic conducting profiles of composite cathode. For example, decrease in the discharge capacity for the Li_{1.1}CoPO₄ and Li_{1.2}CoPO₄ phases noted which is due to the presence of a large amount of Li₃PO₄ phase. Similar kind of variation in the discharge capacity profiles were noted for non-stoichiometric proportions of Li_xMnPO₄ by Whittingham and co-workers.³⁶ The cycling profiles were recorded for up to 25 cycles in galvanostatic mode to analyze the behavior of the samples in conventional electrolytes. These cycling profiles clearly indicate that the lithium rich phase cathodes experience capacity fading during the charge/discharge process. After the 15th cycle, the battery performance of the prepared lithium rich phase materials is slightly better than that of the stoichiometric LiCoPO₄ compound. Among the rich phase materials, Li_{1.05}CoPO₄ and Li_{1.1}CoPO₄ performed slightly better than the other ones. Based on the purity and cell performances of the lithium rich phase compounds, it was determined that Li_{1.05}CoPO₄ exhibits the best battery performance. Finally, we confirmed that the

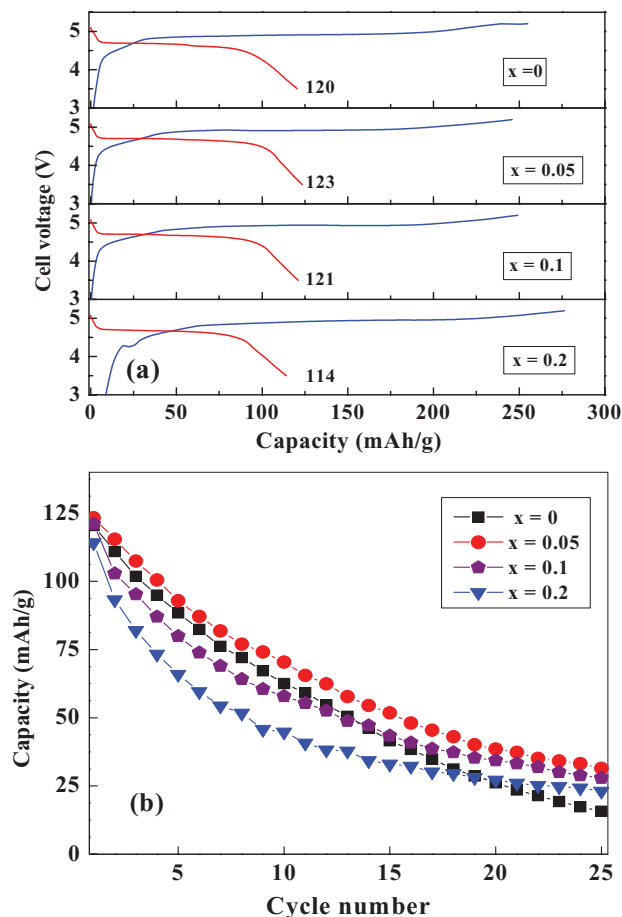


Figure 6. (a) Initial charge-discharge traces of $\text{Li/Li}_{1+x}\text{CoPO}_4$, $0 \leq x \leq 0.2$ cells recorded 3.5–5.2 V at 0.1 C galvanostatically (LiCoPO_4 , $\text{Li}_{1.05}\text{CoPO}_4$, $\text{Li}_{1.1}\text{CoPO}_4$ and $\text{Li}_{1.2}\text{CoPO}_4$), (b) corresponding cycling profiles of the above cells.

real lithium content of the $\text{Li}_{1.05}\text{CoPO}_4$ compound is 1.02 by ICP analysis (it will be described as $\text{Li}_{1.02}\text{CoPO}_4$ hereafter) and this compound was further subjected to Fe substitution into the cobalt sites to improve its cycle performance.

Fe substitution into the $\text{Li}_{1.02}\text{CoPO}_4$ material was successfully carried out at 800°C under the above mentioned conditions. Figure 7 shows the X-ray diffraction patterns of the Fe substituted

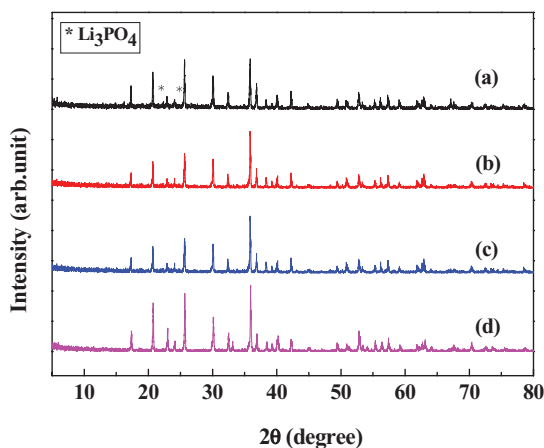


Figure 7. Powder X-ray diffraction patterns of Fe substituted lithium rich cobalt phosphates ($\text{Li}_{1.02}\text{Co}_{1-x}\text{Fe}_x\text{PO}_4$, $0 \leq x \leq 0.2$) prepared at 800°C , (a) $\text{Li}_{1.02}\text{CoPO}_4$, (b) $\text{Li}_{1.02}\text{Co}_{0.95}\text{Fe}_{0.05}\text{PO}_4$ (c) $\text{Li}_{1.02}\text{Co}_{0.9}\text{Fe}_{0.1}\text{PO}_4$ and (d) $\text{Li}_{1.02}\text{Co}_{0.8}\text{Fe}_{0.2}\text{PO}_4$.

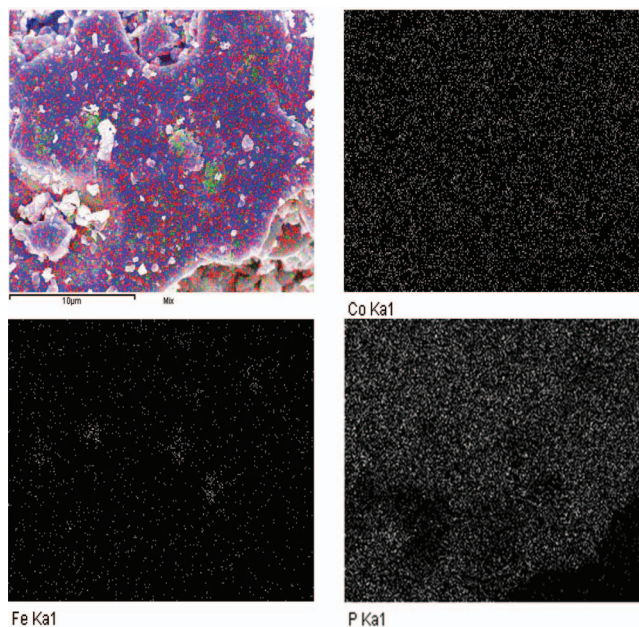


Figure 8. Combined mapping of Co, Fe and P elements, in which Red-Cobalt, Blue-Phosphorous and Green-Iron, and Individual mapping pictures of the above elements.

$\text{Li}_{1.02}[\text{Co}_{1-y}\text{Fe}_y]_{0.98}\text{PO}_4$ ($0 \leq y \leq 0.2$). The absence of Fe peaks in the XRD pattern indicates the formation of $\text{Li}_{1.02}[\text{Co}_{1-y}\text{Fe}_y]_{0.98}\text{PO}_4$ phase. However, the appearance of a meager amount of Li_3PO_4 impurity phase occurred in all of the Fe substituted lithium rich cobalt phosphates. The amount of Fe substitution is too little for it to be detected through X-ray diffraction and, hence, elemental mapping was conducted to ensure the presence of Fe in the $\text{Li}_{1.02}[\text{Co}_{1-y}\text{Fe}_y]_{0.98}\text{PO}_4$ ($0 \leq y \leq 0.2$) matrix, for example, $\text{Li}_{1.02}[\text{Co}_{0.9}\text{Fe}_{0.1}]_{0.98}\text{PO}_4$, and the results are given in Figure 8. The mapping of Fe, Co and P elements clearly demonstrated their presence in the compound. The presence of Co and P is observed throughout the area mapped, whereas the presence of Fe could be partially detected only in a few spots, due to the small amount of the transition metal, Fe, in the above compound. Similar to the previous sections, $\text{Li/Li}_{1.02}[\text{Co}_{1-y}\text{Fe}_y]_{0.98}\text{PO}_4$ ($0 \leq y \leq 0.2$) cells were made to study the electrochemical properties of the prepared materials.

It is well known that transition metal ion doping partially improves the electronic conductivity of olivine phase materials, as reported for LiFePO_4 .³² In the same manner, Kishore and Varadaraju³⁷ employed the substitution of different isovalent ions (Mg, Mn and Ni) into the Co sites and an improvement in the electronic conductivity was noticed, however, severe capacity fading was also observed ($0 \leq x \leq 0.2$). Wang et al.²⁶ employed aliovalent (V^{3+}) doping into the cobalt sites and, in order to maintain the charge balance, the concentration of $(\text{PO}_4)^{3-}$ anions was simultaneously increased. Furthermore, acetylene black was also incorporated to improve the electrochemical properties of the prepared compound under vacuum conditions. They prepared the resultant compound in the absence of Co_2P , however the formation of $\text{Li}_3\text{V}_2(\text{PO}_4)_3$ was inevitable. Further, the $\text{Li}_3\text{V}_2(\text{PO}_4)_3$ phases were much more prevalent in the prepared phase. Recently, Han et al.³⁸ reported that Fe doping into the cobalt sites improves the electrochemical performance of the cell and facilitates the Li^+ diffusivity through the expansion of the 1D channels in the polyanion structure of LiCoPO_4 . Unfortunately, no cycling profiles were reported in the case of Fe doping in this study.³⁶

In this scenario, we adopted Fe doping in the lithium rich phase, $\text{Li/Li}_{1.02}\text{CoPO}_4$, to improve the battery performance. In order to determine the effect of Fe substitution on the battery performance of the $\text{Li/Li}_{1.02}[\text{Co}_{1-y}\text{Fe}_y]_{0.98}\text{PO}_4$ ($0 \leq y \leq 0.2$) cells, cycling tests were carried out at room temperature between 3.5–5.2 V at 0.1 C

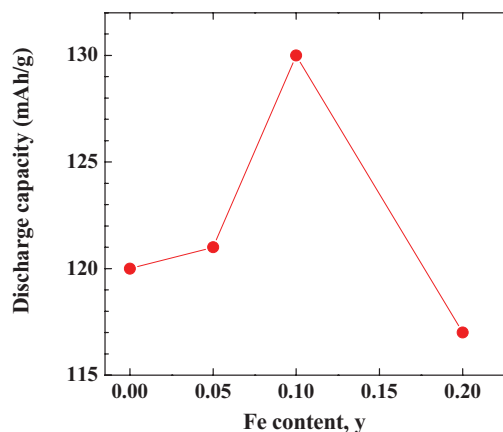


Figure 9. Plot of initial discharge capacity vs. molar concentration of Fe substitution in $\text{Li}_{1.02}[\text{Co}_{1-y}\text{Fe}_y]_{0.98}\text{PO}_4$ phase materials.

rate. The influence of the concentration of Fe substitution on the $\text{Li}_{1.02}[\text{Co}_{1-y}\text{Fe}_y]_{0.98}\text{PO}_4$ is displayed in Figure 9. This figure clearly shows that increasing the concentration of Fe ($y = 0.05$ to 0.1) leads to the enhancement of the cell performance (120 to 130 mAh g^{-1}) up to a concentration of $y = 0.1$. When the concentration exceeds the limit of $y = 0.1$, the suppression of the discharge capacity (117 mAh g^{-1}) occurs in the initial cycle. From the electrochemical properties of the $\text{Li}/\text{Li}_{1.02}[\text{Co}_{1-y}\text{Fe}_y]_{0.98}\text{PO}_4$ ($0 \leq y \leq 0.2$) cells, we found that Fe ion metal substitution in the $\text{Li}_{1.02}\text{CoPO}_4$ matrix is effective in improving the initial discharge capacity and confirmed that the highest value (130 mAh g^{-1}) is observed when the Fe content is 0.1 .

In order to investigate the powder properties of $\text{Li}_{1.02}[\text{Co}_{0.9}\text{Fe}_{0.1}]_{0.98}\text{PO}_4$, which presented the best electrochemical performance during the charge/discharge process, a Rietveld analysis of this material was conducted. Table I shows the refined structural information of LiCoPO_4 and $\text{Li}_{1.02}[\text{Co}_{0.9}\text{Fe}_{0.1}]_{0.98}\text{PO}_4$ using X-ray diffraction. In the case of $\text{Li}_{1.02}[\text{Co}_{0.9}\text{Fe}_{0.1}]_{0.98}\text{PO}_4$, deficient values of the transition metal (TM) occupancies in the 4c site were observed. The lattice parameters of LiCoPO_4 and $\text{Li}_{1.02}[\text{Co}_{0.9}\text{Fe}_{0.1}]_{0.98}\text{PO}_4$ were confirmed by XRD along with the previously reported values for LiCoPO_4 . The lattice parameters were ($a = 10.1931$ (3) Å, $b = 5.9147$ (2) Å, $c = 4.6941$ (1) Å with $R_{\text{wp}} = 20.3\%$ for LiCoPO_4 and $a = 10.196$ (2) Å, $b = 5.919$ (1) Å, $c = 4.6967$ (8) Å with $R_{\text{wp}} = 17.4\%$ for $\text{Li}_{1.02}[\text{Co}_{0.9}\text{Fe}_{0.1}]_{0.98}\text{PO}_4$. The lattice parameters of $\text{Li}_{1.02}[\text{Co}_{0.9}\text{Fe}_{0.1}]_{0.98}\text{PO}_4$ are slightly larger than those of LiCoPO_4 due to the larger ionic size of the doped Fe^{2+} (0.78 Å, high spin) compared with that of Co^{2+} (0.745 Å, high spin).

The cycling profiles of the $\text{Li}/\text{Li}_{1.02}[\text{Co}_{1-y}\text{Fe}_y]_{0.98}\text{PO}_4$ ($0 \leq y \leq 0.2$) cells are given in Figure 10. From the cycling studies it can be seen that, at the end of the 15th cycle of the $\text{Li}_{1.02}[\text{Co}_{1-y}\text{Fe}_y]_{0.98}\text{PO}_4$, the compounds delivered discharge capacities of 42, 47, 117 and 52 mAh g^{-1} for 0, 0.05, 0.1 and 0.2 moles of Fe, respectively. These cycling results suggest that the $\text{Li}_{1.02}[\text{Co}_{0.9}\text{Fe}_{0.1}]_{0.98}\text{PO}_4$ compound

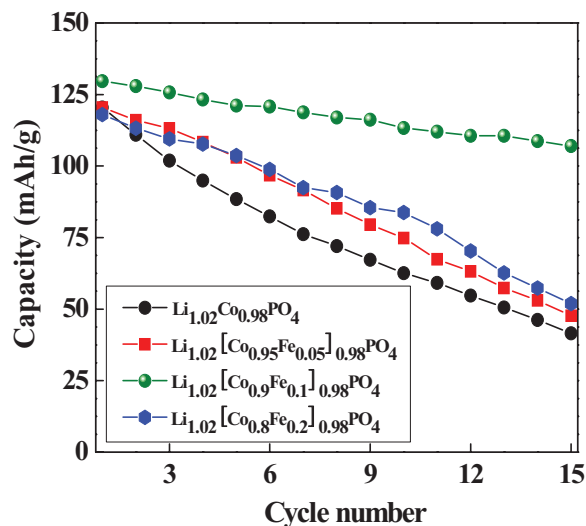


Figure 10. Galvanostatic cycling profiles of $\text{Li}_{1.02}\text{Co}_{1-x}\text{Fe}_x\text{PO}_4$ ($0 \leq x \leq 0.2$) phase materials recorded between 3.5–5.2 V at 0.1 C in room temperature.

retains 90% of its initial discharge capacity at the end of the 15th cycle using a conventional LiPF_6 based electrolyte under the optimized test conditions. To the best of our knowledge, this is one of the best results obtained so far for LiCoPO_4 materials. As expected, the cells with a higher Fe concentration (>0.1) in the lithium cobalt phosphates showed poor performance, but better cell performance than those with the other prepared materials. Furthermore, this result is in good agreement with the results reported by Han et al.³⁸ for Fe doping and indicates that Fe doping facilitates the diffusion of Li^+ ions into the host matrix.

Cyclic voltammetry (CV) was performed to study the kinetic properties of the different cobalt phosphates. The typical CV traces of pure LiCoPO_4 and $\text{Li}_{1.02}[\text{Co}_{0.9}\text{Fe}_{0.1}]_{0.98}\text{PO}_4$ are given in Figure 11. In the CV measurements, metallic lithium served as the counter and reference electrodes with a scan rate of $50 \mu\text{V s}^{-1}$ between (open circuit voltage) ~ 2.8 and 5.2 V in conventional electrolytes. It can be seen from the CV traces that the $\text{Li}_{1.02}[\text{Co}_{0.9}\text{Fe}_{0.1}]_{0.98}\text{PO}_4$ electrode exhibits sharper and more symmetric oxidation and reduction peaks than those of pristine LiCoPO_4 . These more intense and sharp peaks represent the faster diffusion of Li^+ ions on the crystal lattice. The symmetric behavior signifies the excellent reversibility of the Li^+ ions during the redox process. On the other hand, LiCoPO_4 exhibits entirely different redox couples from $\text{Li}_{1.02}[\text{Co}_{0.9}\text{Fe}_{0.1}]_{0.98}\text{PO}_4$ in the sense that broadened peaks are observed, which indicates sluggish kinetic behavior during the reversible insertion of the lithium ions. From these CV measurements, we concluded that transition metal ion doping in the cobalt sites and creating a lithium rich phase improved the electrochemical insertion and extraction of lithium ions during the cycling process.

Table I. Structural information of LiCoPO_4 and $\text{Li}_{1.02}[\text{Co}_{0.9}\text{Fe}_{0.1}]_{0.98}\text{PO}_4$ using Rietveld refinement of X-ray diffraction patterns.

			LiCoPO_4	$\text{Li}_{1.02}[\text{Co}_{0.9}\text{Fe}_{0.1}]_{0.98}\text{PO}_4$
Occupation ratio	4c site	Li	–	0.02
	4c site	Co	1.0	0.884 (4)
	4c site	Fe	–	0.098 (4)
Lattice parameter (Å)	<i>a</i>	10.1931 (3)	10.196 (2)	
	<i>b</i>	5.9147 (2)	5.919 (1)	
	<i>c</i>	4.6941 (1)	4.6967 (8)	
Average transition metal valence	Fe	–	2.05 (4)	
	Co	1.82 (2)	1.83 (4)	

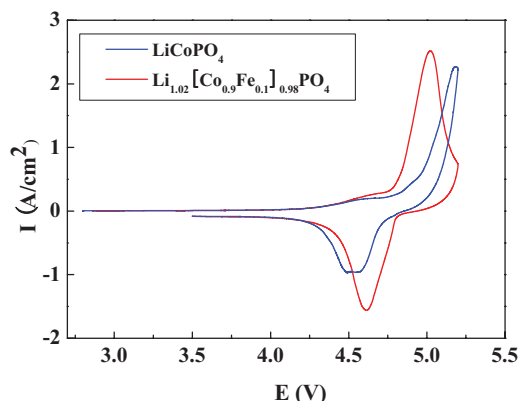


Figure 11. Cyclic voltammograms of Li/LiCoPO₄ and Li/Li_{1.02}Co_{0.9}Fe_{0.1}PO₄ half cells recorded between ~2.8–5.2 V at 0.05 mV s⁻¹, in the above measurements, metallic lithium serves as counter and reference electrode in 1 M LiPF₆ in EC:DMC (1:1 v/v) solution.

Conclusion

The solid state reaction was employed to optimize various olivine lithium cobalt phosphate materials. Based on their structure aspect (XRD) and electrochemical performance, the optimum temperature for the preparation of phosphates was decided to calcine at 800°C in Ar atmosphere. In terms of its purity and electrochemical lithium cycleability, the lithium rich cobalt phosphate (Li_{1.02}CoPO₄, real content) was subjected to further transition metal doping (Fe) in the cobalt sites. Among the various lithium rich Fe doped compounds, the Li_{1.02}[Co_{0.9}Fe_{0.1}]_{0.98}PO₄ phase exhibited better cell performance than the others. The Li/Li_{1.02}[Co_{0.9}Fe_{0.1}]_{0.98}PO₄ cell delivered a capacity of 130 mAh g⁻¹ and retained 90% of its initial discharge capacity (117 mAh g⁻¹) at the end of the 15th cycle. This improved performance is attributed to the increase in the conducting properties via the creation of a lithium rich phase and Fe doping into the cobalt sites. The electrochemical reversibility of the above compound was confirmed by CV measurements.

Acknowledgments

This work was supported by Energy Efficiency and Resources R&D program(2011201010016C) under the Ministry of Knowledge Economy, Republic of Korea.

References

1. A. K. Padhi, K. S. Nanjundaswamy, and J. B. Goodenough, *Journal of the Electrochemical Society*, **144**, 1188 (1997).
2. W. S. Kim, S. B. Kim, I. C. Jang, H. H. Lim, and Y. S. Lee, *Journal of Alloys and Compounds*, **492**, L87 (2010).
3. I. C. Jang, H. H. Lim, S. B. Lee, K. Karthikeyan, V. Aravindan, K. S. Kang, W. S. Yoon, W. I. Cho, and Y. S. Lee, *Journal of Alloys and Compounds*, **497**, 321 (2010).
4. S. B. Lee, S. H. Cho, V. Aravindan, H. S. Kim, and Y. S. Lee, *Bulletin of the Korean Chemical Society*, **30**, 2223 (2009).
5. S. B. Lee, S. H. Cho, J. B. Heo, V. Aravindan, H. S. Kim, and Y. S. Lee, *Journal of Alloys and Compounds*, **488**, 380 (2009).
6. S. B. Lee, I. C. Jang, H. H. Lim, V. Aravindan, H. S. Kim, and Y. S. Lee, *Journal of Alloys and Compounds*, **491**, 668 (2010).
7. H. H. Lim, I. C. Jang, S. B. Lee, K. Karthikeyan, V. Aravindan, and Y. S. Lee, *Journal of Alloys and Compounds*, **495**, 181 (2010).
8. C. G. Son, H. M. Yang, G. W. Lee, A. R. Cho, V. Aravindan, H. S. Kim, W. S. Kim, and Y. S. Lee, *Journal of Alloys and Compounds*, **509**, 1279 (2011).
9. Z. Li, D. Zhang, and F. Yang, *Journal of Materials Science*, **44**, 2435 (2009).
10. D. K. Kim, H. M. Park, S. J. Jung, Y. U. Jeong, J. H. Lee, and J. J. Kim, *Journal of Power Sources*, **159**, 237 (2006).
11. P. S. Herle, B. Ellis, N. Coombs, and L. F. Nazar, *Nature Materials*, **3**, 147 (2004).
12. <http://www.a123systems.com>.
13. <http://www.sony.net/SonyInfo/News/Press/200908/09-083E/index.html>.
14. G. Li, H. Azuma, and M. Tohda, *Electrochemical and Solid-State Letters*, **5**, A135 (2002).
15. S. K. Martha, B. Markovsky, J. Grinblat, Y. Gofer, O. Haik, E. Zinigrad, D. Aurbach, T. Drezen, D. Wang, G. Deghenghi, and I. Exnar, *Journal of the Electrochemical Society*, **156**, A541 (2009).
16. D. Wang, H. Buqa, M. Crouzet, G. Deghenghi, T. Drezen, I. Exnar, N. H. Kwon, J. H. Miners, L. Poletto, and M. Grätzel, *Journal of Power Sources*, **189**, 624 (2009).
17. K. Karthikeyan, V. Aravindan, S. B. Lee, I. C. Jang, H. H. Lim, G. J. Park, M. Yoshio, and Y. S. Lee, *Journal of Alloys and Compounds*, **504**, 224 (2010).
18. T. Shiratsuchi, S. Okada, T. Doi, and J. i. Yamaki, *Electrochimica Acta*, **54**, 3145 (2009).
19. D. S. Su and R. Schlögl, *ChemSusChem*, **3**, 136 (2010).
20. I. C. Jang, H. H. Lim, S. B. Lee, K. Karthikeyan, V. Aravindan, K. S. Kang, W. S. Yoon, W. I. Cho, and Y. S. Lee, *Journal of Alloys and Compounds*, **497**, 321 (2010).
21. K. C. Patil, M. S. Hegde, T. Rattan, and S. T. Aruna, 'Chemistry of nanocrystalline oxide materials: combustion synthesis, properties and applications', World Scientific, Singapore, 2008.
22. K. Amine, H. Yasuda, and M. Yamachi, *Electrochemical and Solid-State Letters*, **3**, 178 (2000).
23. S. Okada, S. Sawa, M. Egashira, J. I. Yamaki, M. Tabuchi, H. Kageyama, T. Konishi, and A. Yoshino, *Journal of Power Sources*, **97-98**, 430 (2001).
24. J. M. Lloris, C. Peñérez Vicente, and J. L. Tirado, *Electrochemical and Solid-State Letters*, **5**, A234 (2002).
25. S. Okada, S. I. Sawa, Y. Uebou, M. Egashira, J. I. Yamaki, M. Tabuchi, H. Kobayashi, K. Fukumi, and H. Kageyama, *Electrochemistry*, **71**, 1136 (2003), <http://sciencelinks.jp/j-east/article/200403/000020040304A0003399.php>.
26. F. Wang, J. Yang, Y. NuLi, and J. Wang, *Journal of Power Sources*, **195**, 6884 (2010).
27. A. Eftekhari, *Journal of the Electrochemical Society*, **151**, A1456 (2004).
28. V. Aravindan, J. Gnanaraj, S. Madhavi, and H.-K. Liu, *Chemistry – A European Journal*, **17**, 14326 (2011).
29. J. Yang and J. J. Xu, *Journal of the Electrochemical Society*, **153**, A716 (2006).
30. H. H. Li, J. Jin, J. P. Wei, Z. Zhou, and J. Yan, *Electrochemistry Communications*, **11**, 95 (2009).
31. J. Wolfenstine, J. Read, and J. L. Allen, *Journal of Power Sources*, **163**, 1070 (2007).
32. S. Y. Chung, J. T. Bloking, and Y. M. Chiang, *Nature Materials*, **1**, 123 (2002).
33. B. Jin, H. B. Gu, and K. W. Kim, *Journal of Solid State Electrochemistry*, **12**, 105 (2008).
34. M. E. Rabanal, M. C. Gutierrez, F. Garcia-Alvarado, E. C. Gonzalo, and M. E. Arroyo-de Dompablo, *Journal of Power Sources*, **160**, 523 (2006).
35. I. C. Jang, C. G. Son, S. M. G. Yang, J. W. Lee, A. R. Cho, V. Aravindan, G. J. Park, K. S. Kang, W. S. Kim, W. I. Cho, and Y. S. Lee, *Journal of Materials Chemistry*, **21**, 6510 (2011).
36. J. Xiao, N. A. Chernova, S. Upreti, X. Chen, Z. Li, Z. Deng, D. Choi, W. Xu, Z. Nie, G. L. Graff, J. Liu, M. S. Whittingham, and J.-G. Zhang, *Physical Chemistry Chemical Physics*, **13**, 18099 (2011).
37. M. V. V. M. S. Kishore and U. V. Varadaraju, *Materials Research Bulletin*, **40**, 1705 (2005).
38. D. W. Han, Y. M. Kang, R. Z. Yin, M. S. Song, and H. S. Kwon, *Electrochemistry Communications*, **11**, 137 (2009).